Rapid resistance evolution against phage cocktails

Baltus A van der Steen[1,3], Matti Gralka[2,3,*], Yuval Mulla[1,3,*]

1. Molecular Microbiology Section, A-LIFE, Vrije Universiteit, 1081 BT Amsterdam, The Netherlands
2. System Biology Section, A-LIFE, Vrije Universiteit, 1081 BT Amsterdam, The Netherlands
3. Amsterdam Institute of Molecular and Life Sciences (AIMMS), Vrije Universiteit, 1081 BT Amsterdam, The Netherlands

* Correspondence: m.gralka@vu.nl, y.mulla@vu.nl

When bacteria are treated with multiple antibiotics simultaneously, resistance is highly unlikely to evolve. In stark contrast, resistance against multiple phages frequently arises during therapy. Why does resistance against multi-phage cocktails evolve so easily? Using a mathematical model, we show how the bacterial evolutionary dynamics and phage replicative dynamics uniquely intertwine, facilitating the rapid evolution of multi-phage resistance. As different phages replicate and become inhibitory at varying time points, bacteria can sequentially acquire resistance rather than simultaneously – increasing the chance of multi-resistance by orders of magnitude. Additionally, we predict and experimentally verify a regime where multi-phage resistance is robustly prevented. Our findings provide a framework for the rational design of phage cocktails to curtail resistance development. Resistance can be minimized by reducing the dose of the most potent phages or by using phages with longer latent periods, as this helps synchronize multi-phage selection.

Bacteriophages are viruses that obligately parasitize bacteria, providing a highly specific mechanism of action that spares the host's commensal microbiota[1]. Although initially developed in the early 20th century and utilized extensively before the antibiotic era, phage therapy was largely sidelined in Western medicine following the mass production of broad-spectrum antibiotics[2]. The global rise of multidrug-resistant 'superbugs' has led to a clinical renaissance for phages, with recent retrospective studies reporting success rates as high as 77.2% in difficult-to-treat cases[4]. However, resistance to therapeutic phages often arises during treatment[4]. To delay or prevent resistance, therapy typically uses cocktails of multiple phages[5]. Classical evolutionary theory predicts that the chance of a resistant mutant decreases exponentially with the number of inhibitory compounds[6] underpins the success of multidrug therapies against diseases like HIV/AIDS[7], tuberculosis[8] and cancer[9]. For example, monotherapy for HIV/AIDS using either protease inhibitors or nucleoside analogues proved ineffective as resistance emerged rapidly[10]; however, their combination is highly effective because it is exponentially more difficult for the pathogen to simultaneously evolve resistance against multiple compounds with distinct mechanisms[11]. This exponential scaling of the chance of resistance with the number of compounds is typically implicitly[12] and sometimes explicitly[13–15] assumed to be true for phages as well - suggesting that resistance evolution should be near-impossible when multi-phage cocktails are used for therapy.

In stark contrast to this prediction, resistance against all components of a multi-phage cocktail is frequently observed during therapy[4, 12], suggesting that multi-phage resistance evolves much more rapidly than predicted by current evolutionary theory.

We show that this contradiction is resolved by accounting for a key difference between phages and conventional drugs: phages replicate, uniquely coupling population dynamics with resistance evolution. To study this combination of phage population dynamics and resistance evolution, we first develop a minimal model of phage therapy with multiple phages against a single pathogen. We show that the probability of resistance evolution hinges on whether two phages act roughly simultaneously to quickly eradicate the host, preventing resistance evolution before population collapse. We then confirm our model predictions experimentally using different sets of phages that either do or do not act simultaneously. Together, our results explain why multi-resistance emerges during phage therapy with cocktails and provides a framework for developing phage cocktails less prone to resistance evolution during treatment.

Methods

Model

To maximize the generality and tractability of our model, we use a deliberately minimalistic model of phage predation. Consistent with previous approaches[16, 17], we model strictly lytic phages adsorb to and burst bacteria, releasing several new phage particles, which can start subsequent infection cycles. Bacteria grow in a steady state and can spontaneously evolve resistance. The number of bacteria that is sensitive to all phages, b_0, grows at a rate μ and spontaneously evolves resistance against phage i (p_i) at a rate r_i. We include predation by phage i, which adsorbs to bacteria at a rate $b_0 k_{\text{adsorb},i}$:

$$\frac{db_0}{dt} = b_0(\mu_0 - \Sigma_{i=1}^{N} r_i) - \Sigma_{i=1}^{N}(p_i b_0 k_{\text{adsorb},i}) \tag{1}$$

Next, we model the population dynamics of bacteria resistant to phage j (b_j) and sensitive to all other phages. For simplicity, we do not consider resistance tradeoffs or phage (co-)evolution:

$$\frac{db_j}{dt} = b_0 r_j + b_j \mu_j - \Sigma_{i=1,i\neq j}^{N}(p_i b_j k_{\text{adsorb},i}) \tag{2}$$

As our model is continuous and mutants resistant to both phage j and l can have very small population sizes, we only allow for cell doublings if there is at least one double-resistant mutant:

$$\frac{db_{j,l}}{dt} = \begin{cases} b_0 r_j r_l + b_l r_j + b_j r_l & \text{if} \quad b_{j,l} < 0 \\ b_0 r_j r_l + b_l r_j + b_j r_l + b_{j,l}\mu_{j,l} & \text{if} \quad b_{j,l} \geq 1 \end{cases} \tag{3}$$

Bacteria infected by phage j (I_j) burst after a latent period of τ_{latency}:

$$\frac{dI_j}{dt} = \Sigma_{i=1,i\neq j}^{N} p_j b_i k_{\text{adsorb},j} - I_j/\tau_{\text{latency},j} \tag{4}$$

For each burst, n_{burst} phages are released. As bacteria typically evolve resistance via receptor protein mutations, we assume phages do not adsorb to resistant bacteria:

$$\frac{dp_j}{dt} = n_{\text{burst},j} I_j/\tau_{\text{latency},j} - \Sigma_{i=1,i\neq j}^{N} p_j b_i k_{\text{adsorb},j} \tag{5}$$

Lastly, we count the number of independently evolved dual-resistant bacterial mutants independently evolved dual-resistant mutants that have arisen in the population (so neglecting any subsequent divisions):

$$\frac{db_{j,l,\text{de novo}}}{dt} = b_0 r_j r_l + b_l r_j + b_j r_l \tag{6}$$

Next, we approximate the chance that a double-mutant evolves, $p_{b_{j,l}}$. To this end, we calculate the chance of at least one mutation occurring, which follows a Poisson distribution according to the classical result of Luria and Delbruck[18]:

$$p_{b_{j,l}} = 1 - e^{-b_{j,l,\text{de novo}}} \tag{7}$$

With this approach, we can approximate the chance of resistance despite the deterministic nature of the model: solving Eq. 6 yields the average number of double-resistant mutants $b_{j,l}$ and by assuming that the number of double-resistant mutants is exponentially distributed over replicate experiments we can then calculate the chance of at least one double-resistant mutant per experiment using Eq. 7.

The set of differential equations was solved numerically using solve_ivp (scipy 1.11.1, Python 3.11.5) and the collapse time of the bacterial populations was detected using find_peaks (scipy 1.11.1, Python 3.11.5)[19].

Chance of simultaneous selection pressure in a phage cocktail

Our model shows that the likelihood of resistance emerging depends critically on whether two phages exert selection pressures simultaneously or sequentially—a dynamic governed by their kinetic properties and initial concentrations. As more phages are added to a cocktail, the probability increases that at least one pair will exert simultaneous selection pressure.

To quantify this, we estimated the probability that a randomly assembled cocktail of n phages from a biobank of N phages contains at least one pair exerting simultaneous selection pressure. Assuming the number of such synergistic pairs is small relative to the total number of combinations($N(N-1)/2$, the probability can be approximated :

$$p_{\text{simultaneous}} = 1 - (1 - \frac{x}{\binom{N}{2}})^{\binom{n}{2}} = 1 - (1 - \frac{x}{\frac{N(N-1)}{2}})^{\frac{n(n-1)}{2}} \tag{8}$$

The value $\frac{x}{\frac{N(N-1)}{2}}$ depends on the collapse time distribution in the biobank. We calculated this parameter using a previously published dataset[20] that measured collapse times for 69 phages from the publicly available Basel collection[11], all infecting the same laboratory strain of *E. coli* (MG1655) under fixed inoculum conditions. Although this strain is non-pathogenic and the data is from in vitro experiments, to our knowledge it is the only available dataset with collapse times measured consistently across a large number of phages.

Suppl. Fig. 3a shows the distribution of collapse times for the individual phages, and Suppl. Fig. 3b–c illustrate the pairwise differences in collapse times. Assuming a 1-hour window of opportunity to prevent resistance (based on Suppl. Fig. 2), approximately 20% of phage pairs fall within this window (Suppl. Fig. 3). In Fig. 5, we plot Eq. 8 using $\frac{x}{\frac{N(N-1)}{2}} = 20\%$,

corresponding to this empirical estimate for the Basel collection, to show how the probability of simultaneous selection pressure scales with cocktail size.

Bacteria and phage propagation

All experiments were performed using *Escherichia coli* MG1655 carrying the kanamycin-resistant plasmid pCS-λ, which encodes a luciferase-based bioluminescence reporter[21]. Pre-cultures were grown overnight at 30 °C in high salt lysogeny broth (LB) with shaking at 150 rpm for liquid cultures, or on 1.5% LB agar (LBA) plates for solid cultures. Phages p17, p33 and p61 of the Basel collection[22] were propagated on *E. coli* in LB at 30 ºC with shaking (150 rpm) overnight. Phages were purified by chloroform treatment (1:75, v/v)[23], followed by centrifugation at 2800 × g. Phage concentrations were determined by 10-fold serial dilution in LB, followed by spotting of 3 µL droplets onto double-layer LBA plates (0.5% top agar) seeded with *E. coli*.

Resistance frequency assay

Phage resistance frequencies were assessed using double-layer LBA plates. Phage-containing supernatants were mixed with overnight *E. coli* cultures and overlaid onto the bottom LBA layer to test resistance against p17, p33, p61, and their combination. To determine the bacterial inoculum concentration, a 10-fold serial dilution of the *E. coli* culture was plated on LBA and incubated overnight at 30 °C. Colony-forming units (CFUs) were counted to calculate resistance frequencies for each condition[18].

One-step growth curve assay

E. coli was cultured to mid-log phase ($OD_{600} \approx 0.5$), diluted (1:100, v/v) and infected with either phage p17, p33 or p61 (final concentration: 10^5 PFU). After a 5-minute adsorption period, cultures were again diluted 1:100 (v/v) and incubated at 30 °C. Samples were collected every 5 minutes, treated with chloroform (1:75, v/v), and phage concentrations were determined via 10-fold serial dilution and spotting onto double-layer agar plates seeded with *E. coli*[24]. The latent period, τ_{latent}, was estimated by empirically fitting the time-resolved phage concentration $[p]$ with a Hill function ($[p] = p_\infty + \frac{p_\infty - p_0}{1 + (\tau_{\text{latent}}/t)}^n$) using optimize.curve_fit (SciPy 1.13.1) in Python[19].

Single phage growth curve

To quantify phage-induced collapse times at various concentrations, 5-fold serial dilutions of either p17 (3×10^9 PFU/mL), p33 (3×10^{10} PFU/mL) and p61 (6×10^9 PFU/mL) were prepared. *E. coli* was grown to mid-log phase, diluted to an OD_{600} of 0.05 (1.69×10^7 CFU/mL), and infected with each phage dilution (1:200, v/v). Cultures were incubated in a 96-well plate (200 µl/well) at 30 ºC for 48h with double orbital shaking. OD_{600} and bioluminescence (BioTek Synergy HTX Multi Mode Plate Reader) were recorded every 10 minutes to determine the collapse time and any regrowth. Collapse times were extracted from bioluminescence curves using find_peaks (SciPy 1.1.13.1) with a smoothing width of three data points.

Dual-phage cocktail

Phages p17, p33 and p61 were diluted to match the concentrations used in the 5-fold serial dilution series from the individual phage growth curve experiments, resulting in an inoculum concentration range of 10^3-10^7 pfu/ml. For comparison, phage preparations at the Belgian phage therapy center[4] are administered at 10^6-10^7 pfu/ml. However, the effective inoculum concentration at the site of an infection is likely much lower than that of the

preparation administered to a patient. The pharmacokinetics of phage products are still poorly understood and likely differ strongly per type of infection. Therefore, although we use realistic phage cocktail concentrations as a guide, we believe it is not yet possible to quantitatively compare our results to actual phage therapy due to a lack of pharmacokinetic knowledge. *E. coli* was grown to mid-log phase and diluted to an OD_{600} of 0.05. Phages were then combined in a 96-well plate (200 µl/well) in a two-dimensional gradient (checkerboard assay)[25], testing all pairwise combinations of the two dilution series across a 48-hour incubation period with shaking at 30 °C. OD_{600} measurements were taken at 0 h for background subtraction and at 48 h to assess bacterial growth. The background-subtracted OD_{600} values were plotted against the difference in collapse time, as determined from the corresponding single-phage growth curves.

Results and Discussion

Using a minimal mathematical model, we first model a bacterial population exposed to a single type of phage (Methods, Suppl. Table 1, reference [26]). We observe that the bacterial population initially grows seemingly unperturbed by the presence of the phage until, after several hours, the bacterial population suddenly collapses due to phage predation, followed by regrowth driven by resistant mutants (Fig. 1a). The bacterial growth is initially unaffected by the phage titer as most bacteria remain uninfected until phages have replicated to much higher numbers[27]. The timing of the collapse is accelerated as the phage inoculum concentration increases (red to blue), in accordance with empirical observations[20].

We investigate a bacterial population exposed to two distinct phages, differing (for now) only in their inoculum concentrations, and find two qualitatively different regimes. When both phages have similar inoculum concentrations, the population undergoes a single and definitive collapse (Fig. 1b, dark curves). In contrast, if inoculum concentrations differ substantially, we observe two sequential collapses followed by a definitive regrowth: the first due to one phage, the second following regrowth of a single-resistant mutant and subsequent collapse due to the second phage and regrowth of a dual-resistant mutant (Fig. 1b, blue and red curves). We call these two regimes simultaneous and sequential selection, respectively.

We calculate the chance of double-resistant mutants arising by first computing the expected average number of double-resistant mutants per experiment (Method Eq. 6) and then calculating the chance that at least one mutant arises per experiment. In the single-collapse regime (simultaneous selection), the probability of double-resistance emergence (Methods Eq. 7) is very low (<<1%, Fig. 1c) because the host population size declines too rapidly for double mutants to emerge. In contrast, in the double-collapse regime (sequential selection), the chance of escape mutants rapidly increases to near-certainty as double resistance can evolve in steps. Therefore, we conclude that the evolution of multi-phage resistance is only prevented within a window of opportunity to prevent resistance where both phages are selective simultaneously (.Fig. 4).

This window of opportunity to prevent resistance provides an experimentally testable prediction: resistance is prevented only when both phages have a matched collapse timing. We test this prediction using two *Escherichia coli* phages (p33 and p61 of the BASEL collection[22]) with similar collapse times (Supplementary Table 1, column 3 of Ref. [20]) but distinct receptor proteins (Supplementary Table 1, column 28 of Ref. [22]), suggesting different resistance pathways. When exposing the host with only one phage at a time, each phage

194 yields resistance in ~1 per million cells, but dual resistance is undetectable ($<10^{-9}$, Suppl. Fig.
195 2a).

196 Previous work simulating bacterial growth curves[28] has revealed that the collapse times
197 depend on both phage parameters (burst size, adsorption rate, latency time), but also initial
198 phage abundance. Therefore, we systematically vary the inoculum concentrations of each
199 phage across four orders of magnitude and measure bacterial growth after 48 hours. Single
200 phage treatments always result in regrowth, and regrowth is also observed in ⅓ of dual-phage
201 cocktails (Suppl. Fig. 1b) — despite the number of bacteria being much smaller than the
202 inverse frequency of dual resistance (Suppl. Fig. 1a). Closer inspection reveals that successful
203 suppression without regrowth only occurs at high inoculum concentrations of p61 but low
204 inoculum concentrations of p33 (Fig. 2c).This means that an increase in p33's inoculum
205 concentration actually decreases suppression - counterintuitively, because typically, one
206 might expect an increased dosage to lead to greater efficacy. More specifically, we find that
207 resistance is only suppressed when the collapse time of p61 precedes that of p33 (Fig. 2d).

208 Similar to our model prediction (Fig. 1c), we experimentally find that the difference in collapse
209 time is the main determinant for stable suppression of bacterial growth (Fig. 2d). However, in
210 contrast to the predictions of our simple model (Fig. 1c), we do not experimentally observe a
211 window of opportunity to prevent resistance that is symmetric around 0 difference in collapse
212 time. However, that model made the strong assumption that phage parameters were identical
213 between the phages. Lifting this assumption, we find that the window of opportunity to prevent
214 resistance predictably depends on these phage parameters: increases with the phage latent
215 period widen the window (Suppl. Fig. 2) and asymmetry arises when phages have different
216 latent periods. Therefore, resistance is best prevented when the phage with the longer latent
217 period acts first (Fig. 3a). After determining the latent period of p33 and p61 via one-step
218 growth curve experiments, we find that, consistent with our theoretical prediction, p61 (the
219 phage which suppresses regrowth when causing the early collapse) indeed has a longer latent
220 period than p33 (resp. 49±3 min and 37±1 min, $p=10^{-5}$, Fig. 3b, Suppl. Fig. 1c).

221 To understand the mechanism by which the latent period affects the window of opportunity
222 to prevent resistance, we perform simulations of bacteria exposed to a single type of phage,
223 varying the latent period of that phage. These simulations reveal why the latent period is
224 such a relevant parameter: whereas a short latent period causes a steep collapse, a long
225 latent period causes a more gradual collapse (Fig. 3c). Such a gradual collapse broadens
226 the window of opportunity to prevent resistance and allows the second phage to catch up
227 with the phage causing the first collapse.

228 In our experiment, p33 and p61 were carefully chosen for their similar bactericidal activity
229 (comparable collapse times). Indeed, when we choose sets of phages with very dissimilar
230 bactericidal activity (p17 and p61), the robust resistance suppression is only achieved at an
231 extreme inoculum concentration difference (>100x, Suppl. Fig. 4). This shows that, following
232 the prediction, collapse times roughly must coincide for resistance suppression, raising the
233 question how this can be achieved when assembling phage cocktails. To highlight how likely
234 an arbitrary cocktail of phages is to operate within this effective window as a function of the
235 number of phages in a cocktail, we analyzed published collapse-time data from multiple
236 phages infecting *E. coli*[20]. We calculate the likelihood that any two phages within a random
237 cocktail fall within this window (Methods Eq. 7), leading to simultaneous selection. We find
238 that this chance increases roughly linearly for low numbers of phages (Fig. 5), which is

239 qualitatively different from the exponential scaling of chance of resistance for antibiotics[4]. This
240 qualitative difference between antibiotics and phages as bactericidal agents may explain why
241 multi-resistance is more frequently observed during phage therapy than multi-resistance
242 against antibiotic cocktails.

243 Our study explains how multi-phage resistance evolution may differ from that of antibiotics due
244 to the replicative nature of phages and offers an explanation of why multi-phage resistance is
245 a major clinical problem. Although we have only considered de novo mutations, resistance
246 acquired via horizontal gene transfer would follow similar rules as the only alteration would be
247 that the mutation rate then also depends on the density of donor bacteria as reviewed in Ref.
248 [30]. Therefore, multi-phage resistance can be acquired sequentially independent of the mode
249 by which the resistance evolves.

250 In principle, *in vitro* screening could help identify phage pairs that cause similar collapse
251 timings. However, phage pharmacokinetics *in vivo* differ markedly from test tube
252 conditions[31], so predicting collapse timing in patients is difficult. This discrepancy suggests
253 that in vitro cocktail performance should be interpreted with caution; a cocktail's apparent
254 efficacy in a test tube may rely on a specific timing of selection pressure that does not translate
255 to the patient. Our work does show that the initial phage titer controls evolutionary dynamics
256 in non-trivial ways. Therefore, an important next step is to record resistance rates as a function
257 of initial phage titers in more complex infection models (e.g. animal models[32] or
258 organoids[33]) to find optimal regimes.

259 Designing effective phage cocktails requires a rigorous understanding of the evolutionary
260 interplay between constituent phages. For example, resistance to one phage must not confer
261 cross-resistance to others in the mixture[34]. Our findings demonstrate that standard *in vitro*
262 cocktail assays can conflate these fundamental evolutionary interactions with population
263 dynamics, such as collapse timing. Because these timing effects are highly sensitive to
264 pharmacokinetic variations and likely translate poorly to *in vivo* conditions, it is critical to
265 employ diagnostic assays that isolate evolutionary outcomes from ecological noise.
266 Researchers can directly quantify the genetic barriers to multi-phage resistance through
267 sequential exposure, which involves isolating mutants resistant to a primary phage and then
268 challenging them with a secondary agent. Unlike simultaneous cocktail assays[35, 36], these
269 sequential tests[37] are independent of collapse timing and thus provide a more robust
270 assessment of a cocktail's therapeutic potential in clinical settings. Sequential testing reveals
271 cross-resistance patterns[38], but does not ensure a simultaneous selection pressure. To
272 increase the change of simultaneous selection and therefore robust resistance suppression,
273 it is beneficial to further increase the number of distinct phages (Fig. 5) - especially those with
274 longer latent periods (Suppl. Fig. 2b). Finally, resistance does not always imply failure[4, 39]:
275 resistance to phages can increase sensitivity to antibiotics[40] or reduce virulence[41]. These
276 evolutionary trade-offs could be exploited, and some researchers already recommend
277 including them as a criterion in phage selection[42]. Our findings highlight the challenge of
278 fully preventing phage resistance, the importance of better understanding *in vivo* phage
279 pharmacokinetics and the need to integrate evolutionary principles into therapy design.

280 **References**

281 1. Febvre HP et al. PHAGE Study: Effects of Supplemental Bacteriophage Intake on
282 Inflammation and Gut Microbiota in Healthy Adults. *Nutrients* 2019;**11**:666.
283 https://doi.org/10.3390/nu11030666
284 2. Summers WC. The strange history of phage therapy. *Bacteriophage* 2012;**2**:130–133.
285 https://doi.org/10.4161/bact.20757
286 3. Murray CJL et al. Global burden of bacterial antimicrobial resistance in 2019: a
287 systematic analysis. *The Lancet* 2022;**399**:629–655. https://doi.org/10.1016/S0140-
288 6736(21)02724-0
289 4. Pirnay J-P et al. Personalized bacteriophage therapy outcomes for 100 consecutive
290 cases: a multicentre, multinational, retrospective observational study. *Nat Microbiol*
291 2024;1–20.
292 5. Yoo S et al. Designing phage cocktails to combat the emergence of bacteriophage-
293 resistant mutants in multidrug-resistant Klebsiella pneumoniae. *Microbiol Spectr*
294 2023;**12**:e01258-23. https://doi.org/10.1128/spectrum.01258-23
295 6. Wang X et al. Engineered Mycobacterium tuberculosis triple-kill-switch strain provides
296 controlled tuberculosis infection in animal models. *Nat Microbiol* 2025;**10**:482–494.
297 https://doi.org/10.1038/s41564-024-01913-5
298 7. Hammer SM et al. A controlled trial of two nucleoside analogues plus indinavir in
299 persons with human immunodeficiency virus infection and CD4 cell counts of 200 per
300 cubic millimeter or less. AIDS Clinical Trials Group 320 Study Team. *N Engl J Med*
301 1997;**337**:725–733. https://doi.org/10.1056/NEJM199709113371101
302 8. Omoteso OA et al. Innovative Strategies for Combating Multidrug-Resistant
303 Tuberculosis: Advances in Drug Delivery Systems and Treatment. *Microorganisms*
304 2025;**13**:722. https://doi.org/10.3390/microorganisms13040722
305 9. Bock C, Lengauer T. Managing drug resistance in cancer: lessons from HIV therapy.
306 *Nat Rev Cancer* 2012;**12**:494–501. https://doi.org/10.1038/nrc3297
307 10. Larder BA, Kemp SD. Multiple mutations in HIV-1 reverse transcriptase confer high-

308 level resistance to zidovudine (AZT). *Science* 1989;**246**:1155–1158.
309 https://doi.org/10.1126/science.2479983
310 11. Perelson AS et al. HIV-1 dynamics in vivo: virion clearance rate, infected cell life-span,
311 and viral generation time. *Science* 1996;**271**:1582–1586.
312 https://doi.org/10.1126/science.271.5255.1582
313 12. Yang Y et al. Development of a Bacteriophage Cocktail to Constrain the Emergence of
314 Phage-Resistant Pseudomonas aeruginosa. *Front Microbiol* 2020;**11**.
315 https://doi.org/10.3389/fmicb.2020.00327
316 13. Abedon ST, Danis-Wlodarczyk KM, Wozniak DJ. Phage Cocktail Development for
317 Bacteriophage Therapy: Toward Improving Spectrum of Activity Breadth and Depth.
318 *Pharmaceuticals* 2021;**14**:1019. https://doi.org/10.3390/ph14101019
319 14. Oromí-Bosch A, Antani JD, Turner PE. Developing Phage Therapy That Overcomes
320 the Evolution of Bacterial Resistance. *Annu Rev Virol* 2023;**10**:503–524.
321 https://doi.org/10.1146/annurev-virology-012423-110530
322 15. Marchi J et al. Multi-strain phage induced clearance of bacterial infections. *PLOS*
323 *Comput Biol* 2025;**21**:e1012793. https://doi.org/10.1371/journal.pcbi.1012793
324 16. Marchi J et al. The dynamic interplay of bacteriophage, bacteria and the mammalian
325 host during phage therapy. *iScience* 2023;**26**. https://doi.org/10.1016/j.isci.2023.106004
326 17. Levin BR, Bull JJ. Population and evolutionary dynamics of phage therapy. *Nat Rev*
327 *Microbiol* 2004;**2**:166–173. https://doi.org/10.1038/nrmicro822
328 18. Luria SE, Delbrück M. MUTATIONS OF BACTERIA FROM VIRUS SENSITIVITY TO
329 VIRUS RESISTANCE. *Genetics* 1943;**28**:491–511.
330 https://doi.org/10.1093/genetics/28.6.491
331 19. Virtanen P et al. SciPy 1.0: fundamental algorithms for scientific computing in Python.
332 *Nat Methods* 2020;**17**:261–272. https://doi.org/10.1038/s41592-019-0686-2
333 20. Mulla Y et al. Extreme diversity of phage amplification rates and phage–antibiotic
334 interactions revealed by PHORCE. *PLOS Biol* 2025;**23**:e3003065.
335 https://doi.org/10.1371/journal.pbio.3003065

336 21. Kavčič B, Tkačik G, Bollenbach T. Mechanisms of drug interactions between
337 translation-inhibiting antibiotics. *Nat Commun* 2020.
338 22. Maffei E et al. Systematic exploration of Escherichia coli phage–host interactions with
339 the BASEL phage collection. *PLOS Biol* 2021;**19**:e3001424.
340 https://doi.org/10.1371/journal.pbio.3001424
341 23. Sechaud J, Kellenberger E. Early lysis produced by chloroform in bacteria infected by
342 bacteriophage. *Ann Inst Pasteur* 1956;**90**:102–106.
343 24. Ellis EL, Delbrück M. The growth of bacteriophage. *J Gen Physiol* 1939;**22**:365–384.
344 https://doi.org/10.1085/jgp.22.3.365
345 25. Bellio P et al. New and simplified method for drug combination studies by checkerboard
346 assay. *MethodsX* 2021;**8**:101543. https://doi.org/10.1016/j.mex.2021.101543
347 26. Krysiak-Baltyn K et al. Computational models of populations of bacteria and lytic phage.
348 *Crit Rev Microbiol* 2016;**42**:942–968. https://doi.org/10.3109/1040841X.2015.1114466
349 27. Geng Y et al. Using bacterial population dynamics to count phages and their lysogens.
350 *Nat Commun* 2024;**15**:7814. https://doi.org/10.1038/s41467-024-51913-6
351 28. Blazanin M et al. Theoretical validation of growth curves for quantifying phage-bacteria
352 interactions. *BioRxiv* 2023;2023.06.29.546975.
353 29. Wang X et al. Engineered Mycobacterium tuberculosis triple-kill-switch strain provides
354 controlled tuberculosis infection in animal models. *Nat Microbiol* 2025;**10**:482–494.
355 https://doi.org/10.1038/s41564-024-01913-5
356 30. Alderliesten JB et al. Effect of donor-recipient relatedness on the plasmid conjugation
357 frequency: a meta-analysis. *BMC Microbiol* 2020;**20**:135.
358 https://doi.org/10.1186/s12866-020-01825-4
359 31. Nang SC et al. Pharmacokinetics/pharmacodynamics of phage therapy: a major hurdle
360 to clinical translation. *Clin Microbiol Infect* 2023;**29**:702–709.
361 https://doi.org/10.1016/j.cmi.2023.01.021
362 32. Kaito C et al. Animal infection models using non-mammals. *Microbiol Immunol*
363 2020;**64**:585–592. https://doi.org/10.1111/1348-0421.12834

364 33. Blutt SE, Estes MK. Organoid Models for Infectious Disease. *Annu Rev Med*
365 2022;**73**:167–182. https://doi.org/10.1146/annurev-med-042320-023055
366 34. Wright RCT et al. Cross-resistance is modular in bacteria–phage interactions. *PLOS*
367 *Biol* 2018;**16**:e2006057. https://doi.org/10.1371/journal.pbio.2006057
368 35. Penke TJR et al. High-throughput methods leveraging robotics and computer vision for
369 the development of therapeutic phage cocktails. *Nat Commun* 2026.
370 https://doi.org/10.1038/s41467-026-68684-x
371 36. Hall AR et al. Effects of Sequential and Simultaneous Applications of Bacteriophages
372 on Populations of Pseudomonas aeruginosa In Vitro and in Wax Moth Larvae. *Appl*
373 *Environ Microbiol* 2012;**78**:5646–5652. https://doi.org/10.1128/AEM.00757-12
374 37. Kim MK et al. A blueprint for broadly effective bacteriophage-antibiotic cocktails against
375 bacterial infections. *Nat Commun* 2024;**15**:9987. https://doi.org/10.1038/s41467-024-
376 53994-9
377 38. Roemhild R, Bollenbach T, Andersson DI. The physiology and genetics of bacterial
378 responses to antibiotic combinations. *Nat Rev Microbiol* 2022;**20**:478–490.
379 https://doi.org/10.1038/s41579-022-00700-5
380 39. Van Nieuwenhuyse B et al. Bacteriophage-antibiotic combination therapy against
381 extensively drug-resistant Pseudomonas aeruginosa infection to allow liver
382 transplantation in a toddler. *Nat Commun* 2022;**13**:5725.
383 https://doi.org/10.1038/s41467-022-33294-w
384 40. Burmeister AR et al. Pleiotropy complicates a trade-off between phage resistance and
385 antibiotic resistance. *Proc Natl Acad Sci* 2020;**117**:11207–11216.
386 https://doi.org/10.1073/pnas.1919888117
387 41. Castledine M et al. Parallel evolution of Pseudomonas aeruginosa phage resistance
388 and virulence loss in response to phage treatment in vivo and in vitro. *eLife*
389 2022;11:e73679. https://doi.org/10.7554/eLife.73679
390 42. Würstle S et al. Optimized preparation pipeline for emergency phage therapy against
391 Pseudomonas aeruginosa at Yale University. Sci Rep 2024;14:2657.

392 https://doi.org/10.1038/s41598-024-52192-3

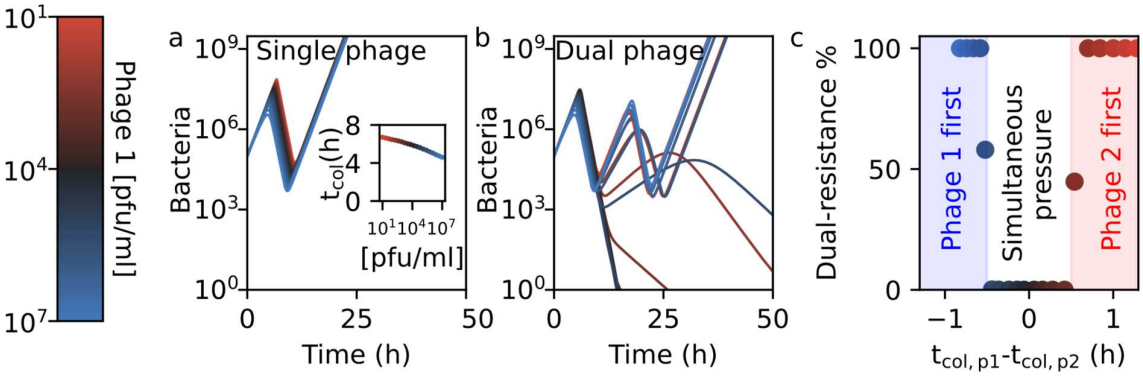

Fig. 1 Theory predicts timing of selection pressure determines the likelihood of multi-phage resistance. a) Simulated bacterial population dynamics under attack from a single phage. Growth initially continues before a sudden collapse and rebound due to resistant mutants. Inset: collapse time as a function of phage inoculum concentration (red to blue, see color bar and inset). **b)** Dynamics under a two-phage cocktail, varying the inoculum concentration of phage 1 (same as in panel a, see color bar), keeping the concentration of phage 2 fixed at 10^4 pfu/ml - with the black line representing equal inoculum concentrations for both phages. Depending on the inoculum concentration of phage 1, phage action can be simultaneous (single collapse in case of the dark lines) or sequential (two collapses in case of the bright red and bright blue lines). **c)** Probability of double-resistance emergence (calculated from simulations in panel b) as a function of the difference in collapse times between the individual phages 1 and 2 (calculated from panel a). Resistance is strongly suppressed only when both phages act simultaneously. All Panels share the same phage inoculum concentration color scale (left).

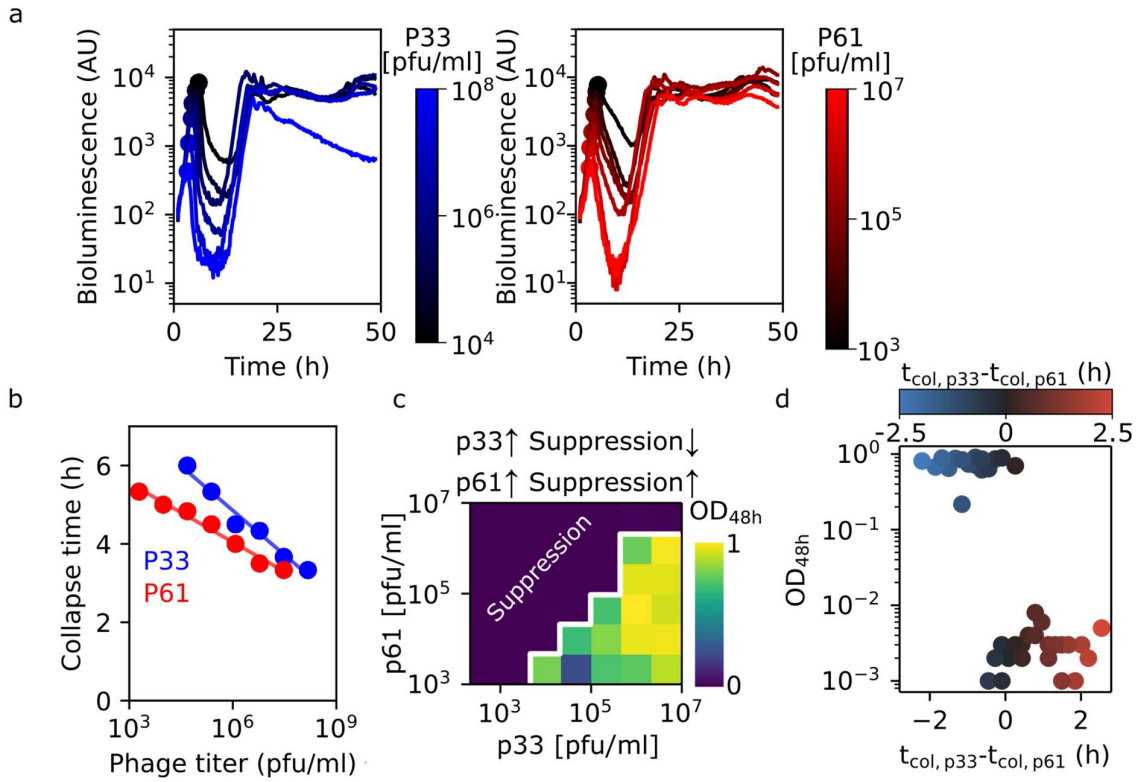

Fig. 2 Experiments confirm timing of selection pressure determines the likelihood of multi-phage resistance. a) Bacterial growth curves at increasing phage concentrations: left panel for p33 (blue to black), right panel for p61 (red to black). **b)** Collapse times derived from growth curves in panel a. **c)** Experimental data showing bacterial growth (optical density after 48 h) is only suppressed when p61 is at high and p33 at low inoculum concentrations, meaning that increasing the inoculum concentration of p33 actually decreases suppression. The white line highlights the sharp transition where phages no longer stably suppress bacterial growth. **d)** The same data as panel c, now plotted against the difference in single-phage collapse time (panel b).

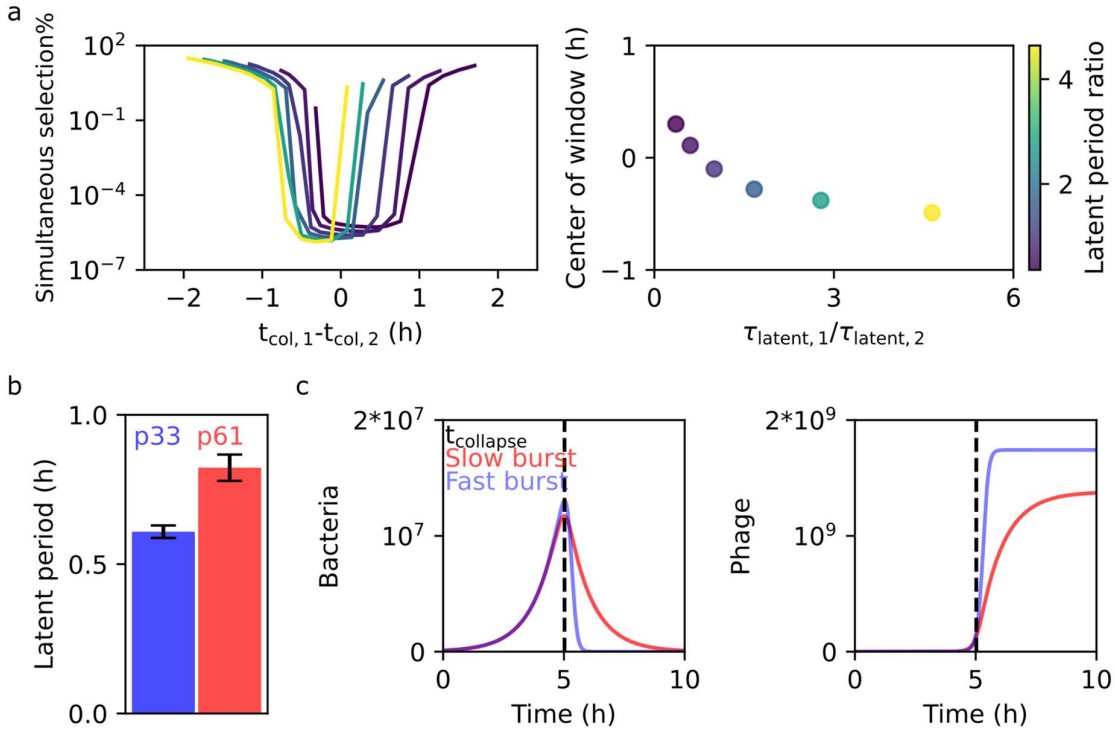

Fig. 3 Resistance is suppressed most when the phage with the longest latent period causes the first collapse. a) Dual-phage simulations with identical burst size and adsorption rate, differing only in their latent period (color bar, see suppl. Table 1 for all parameters). We vary the difference in collapse time (x-axis, left panel) by varying the inoculum concentrations. The theoretical model predicts that the window where resistance is suppressed shifts as a function of the ratio between the latent periods of both phages (right panel), such that resistance is suppressed most when the phage with the longest latent period causes the first collapse. **b)** We experimentally confirm that phage 61, which has to collapse first for efficient resistance suppression (Fig. 1c), indeed has a longer collapse time. The error bar shows the standard deviation of the fit (Suppl. Fig. 1c). **c)** Simulations of single-phage predation assays reveal why the latent period shifts the window of opportunity to prevent resistance. If the latent period is short (blue), then the collapse of the bacterial population (right) and the increase in the phage population (left) are sudden. In contrast, both are more gradual if the latent period is long (red) - shifting the window a second phage can simultaneously suppress growth.

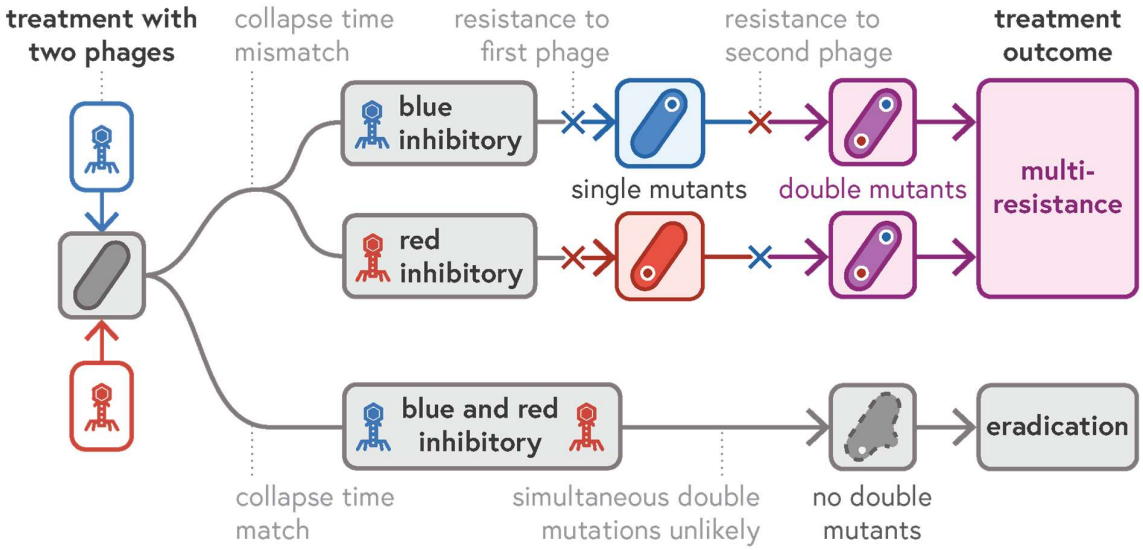

Fig. 4 Schematic of the resistance evolution pathways against phage cocktails. Upon application of a multi-phage cocktail, each phage replicates at its own rate and reaches inhibitory concentrations at different times. If these selective events occur sequentially, resistance can evolve stepwise. Only when multiple phages act simultaneously is the evolution of multi-phage resistance robustly suppressed (bottom).

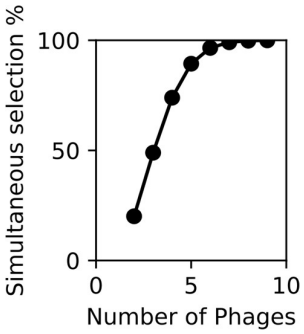

Fig. 5 Complex enough phage cocktails still robustly suppress resistance evolution Simulated probability that at least one phage pair in a cocktail exerts simultaneous selection, plotted as a function of cocktail size and phage latent period. Based on data from a public *E. coli* phage library[20, 22]. Calculations follow Methods Eq. 8. The plot shows that even though multi-phage cocktails are less effective than traditional drugs in suppressing resistance, simultaneous selection pressure (which effectively prevents resistance) can still be achieved by combining enough different phages.

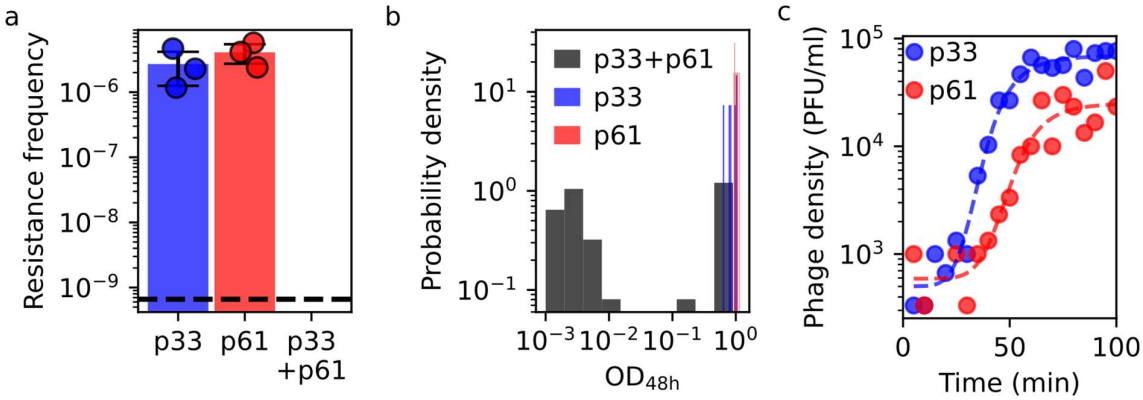

Suppl. Fig. 1 p33 and p61 characterization a) Resistance frequencies for p33 alone (blue), p61 alone (red), and both combined (below detection limit; dashed line). **b)** Final optical density distribution after 48 h for p33 (blue), p61 (red), and the cocktail (grey). **c)** One-step growth curves for p33 and p61.

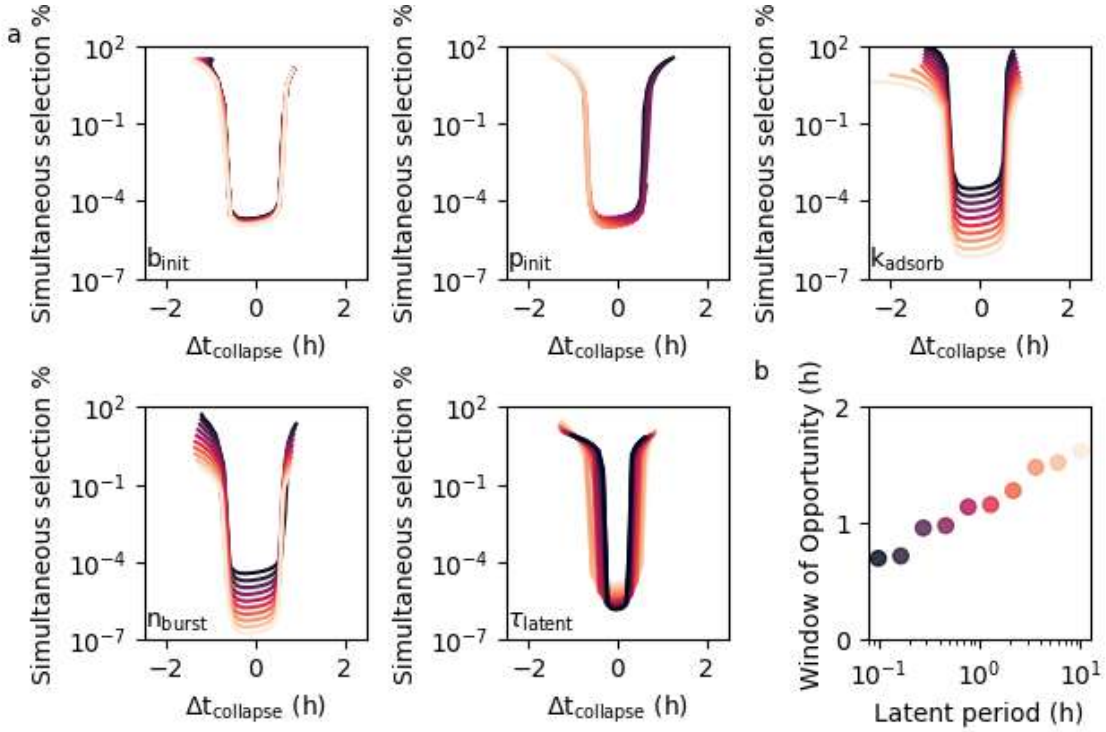

Suppl. Fig. 2 Latent period influences the size and position of the window of opportunity to prevent resistance. Dual-phage simulations using identical phages, varying the inoculum concentration of one phage holding the other constant. Resistance frequency (y-axis) is plotted against the difference in collapse time (x-axis) derived from single-phage simulations. Simulations were run across a range of parameters (different panels) in logarithmic steps (ranging from low in dark to high in bright, see Suppl. Table 1 for the exact ranges). **b)** Wider latent periods increase the window of collapse-time differences over which resistance is suppressed. The color coding reflects the latent period and is the same as in panel a, bottom-right.

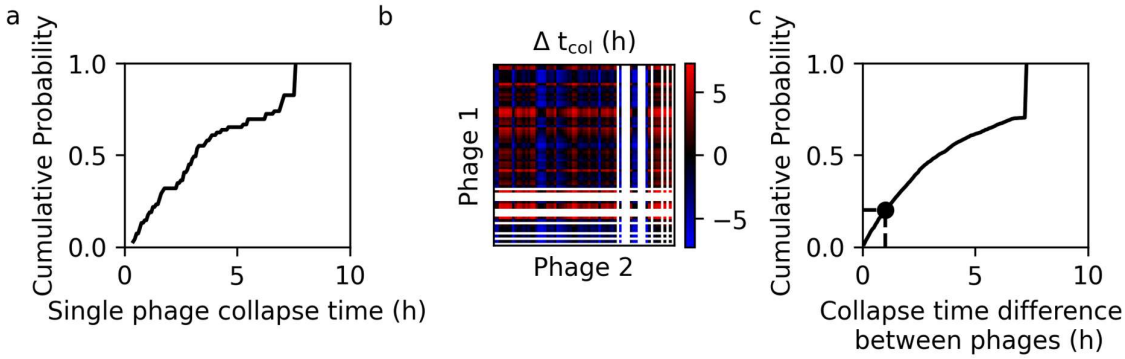

Suppl. Fig. 3 BASEL collection collapse time distribution To estimate how often two phages might act simultaneously and thus prevent resistance, we analyzed published collapse-time data for 69 *E. coli*-infecting phages from the BASEL collection[20]. **a)** Cumulative distribution of collapse times. For 11 of 69 phages, collapse times could not be measured due to very slow lysis dynamics. **b)** Heatmap showing pairwise differences in collapse time for all measurable phage pairs. White lines indicate phages for which collapse times were undetermined. Collapse time differences between specific phage pairs can be found in the Supplementary Data. **c)** Cumulative distribution of collapse-time differences from panel b, excluding the diagonal (self-comparisons). Pairs involving phages with indeterminable collapse times were treated as having infinite differences. ~20% of phage-phage pairs differ by 1 hour or less (dashed line).

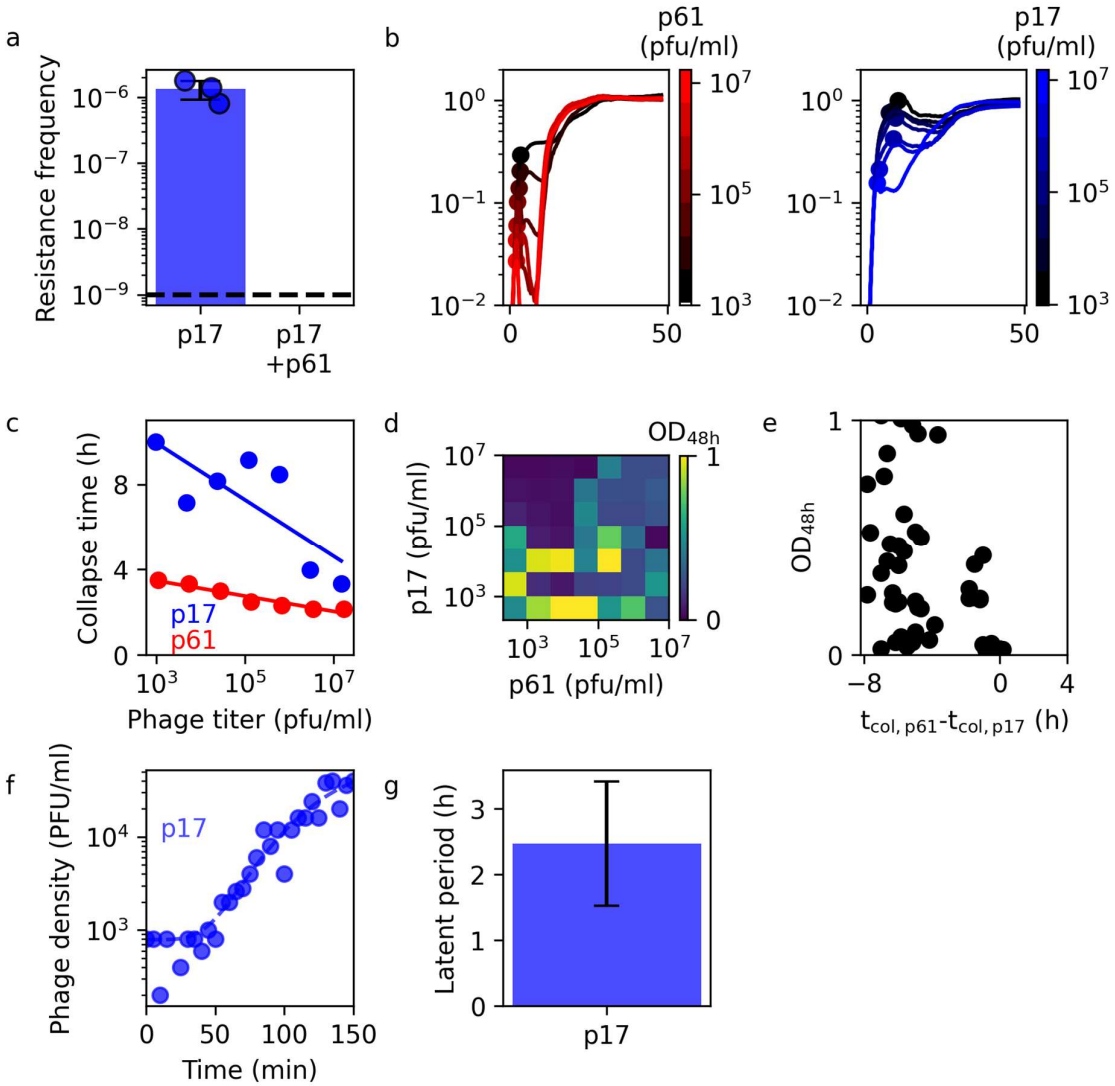

Suppl. Fig. 4 phages with different bactericidal activity only show stable suppression at a large phage inoculum concentration imbalance a) Resistance frequencies for phage 17 alone (blue) or combined with p61 (below detection limit; dashed line, see p61 alone is in Suppl. Fig 1a). The results indicate no collateral resistance between both phages. **b)** Bacterial growth curves at increasing phage concentrations: left panel for p17 (blue to black), right panel for p61 (red to black). **c)** Collapse times derived from growth curves in panel b. **d)** Experimental data showing bacterial growth (optical density after 48 h) is only suppressed when the inoculum concentration of p17 is at least 100x higher than of p61. **e)** The same data from panel c, now plotted against the difference in single-phage collapse time (panel b). **f)** One-step growth curves for p17. **g)** Latent period extracted from the one-step growth curve (panel f). The error bar shows the standard deviation based on the fit.

	b_{init} [cfu]	p_{init} [pfu]	μ [h^{-1}]	k_{adsorb} [h^{-1} cfu^{-1}]	τ_{latency} [h]	n_{burst} [ ]	r []
Fig. 1	10^5	10^1-10^7	1	10^{-8}	1	100	10^{-6}
Suppl. Fig. 3 (fixed)	10^5	10^1-10^7	1	10^{-8}	1	100	10^{-8}
Fig. 3 a, Suppl. Fig. 3 (variable)	10^4-10^6	10^3-10^5	0.2-2	10^{-7}-10^{-9}	0.02-2	50-5000	10^{-8}

Suppl. Table 1 Model parameters used in simulations To explore the impact of different phage traits on resistance evolution, we simulated a dual-phage predation assay in which both phages initially share identical kinetic parameters. Each parameter was varied individually across 10 logarithmically spaced steps, keeping all others constant. To modulate the difference in collapse timing, the inoculum concentration of one phage was varied across 20 logarithmically spaced steps from 10^1 to 10^7 pfu, keeping the concentration of the other fixed at 10^4 pfu.